Multiple Bragg wave coupling in photonic band-gap crystals

Henry M. van Driel[*] and Willem L. Vos[†]

Van der Waals-Zeeman Instituut, Universiteit van Amsterdam, 1018 XE Amsterdam, The Netherlands
(Received 27 January 2000)

We report angle and polarization resolved reflectivity from strongly photonic fcc crystals consisting of air spheres in titania. For a 30° range of angles of incidence, multiple peaks with distinct polarization dependence are observed that clearly reveal avoided crossing behavior. Calculated photonic dispersion curves show that the multiple peaks result from band repulsion of Bloch states due to simultaneous Bragg diffraction by (111) and (200) planes. Our results demonstrate that many-wave coupling leads to substantial deviations from simple Bragg diffraction, with significantly flattened bands, a requirement for the appearance of complete photonic band gaps.

Photonic crystals have become an increasingly important focus of fundamental and applied science following the pioneering suggestions for their existence.[1,2] These three-dimensional (3D) dielectric lattices, with periodicity on the order of an optical wavelength, manipulate light through Bragg diffraction and photonic dispersion bands,[3,4] just as semiconductor crystals control electrons.[5] Photonic materials have already led to exciting developments such as efficient light sources,[6] superprisms,[7] and miniature laser cavities.[8] A major research objective is the attainment at optical frequencies of a photonic band-gap—a range of frequencies for which Bragg reflections inhibit light propagation for *all* directions and polarizations. The ensuing gap in the photon density of states promises novel physical phenomena such as light localization and inhibited spontaneous emission.[1]

In simple Bragg diffraction, the resonance wavelength is governed by the crystal plane spacing and angle of incidence, and the diffraction bandwidth increases with the spatial contrast between the dielectric constants.[9] Photonic band gaps are expected in strongly photonic crystals (crystals with high dielectric contrast), because Bragg reflection bands from many differently oriented crystal planes overlap. The multiple diffraction induces marked coupling effects, causing the dispersion relations to become strongly modified relative to simple Bragg diffraction. Surprisingly, there have been no[10] investigations of multiple Bragg diffraction in photonic crystals, an effect which holds the key to understanding how band-gaps form. Strongly photonic crystals have been realized in Ref. 11, but the samples are typically only a few unit cells thick, hence finite size effects probably overwhelm multiple Bragg reflections. Extended 3D crystals made from self-organizing systems interact so weakly with light that multiple Bragg diffraction is easily unnoticed;[12] for strongly photonic inverse opals that inhibit light propagation for >55% of all directions,[13] experimental limitations precluded the observation of multiple Bragg diffraction.[14]

Here, we present angle- and polarization-resolved reflectivity spectra from strongly photonic 3D crystals over wide frequency ranges where avoided crossings typical of coupled modes occur, and observe multiple diffraction peaks. The observations are in excellent agreement with calculations of the dispersion curves for photonic Bloch states resulting from coupled Bragg diffractions by (111)- and (200)-like crystal planes. Optical diffraction in strongly photonic crystals is therefore much more complex than previously considered. As multiple Bragg wave coupling predominates with increasing photonic interaction strength and increasing frequency, it allows for a new understanding of flat dispersion bands, modifications of the density of states, and the formation of photonic band gaps.

The samples studied are fcc crystals of air spheres in titania (TiO_2). General preparation methods for the crystals have been presented earlier.[15] Improved growth techniques have led to high quality crystal domains, see the typical surface in Fig. 1, with diameters as large as ~ 500 μm. The samples have lattice parameter a between 830 and 860 nm, allowing a broad relative spectral range a/λ (λ is the wavelength of light) to be studied.[14] The titania filling fraction was determined to be between 8 and 12 vol. % from x-ray experiments. The optical setup used to measure specular reflection spectra is similar to that described in Ref. 13. The light polarization is controlled with high contrast ($>100:1$) polarizers. A wide spectral range, from 7000 to 22 000 cm^{-1}, is achieved by using tungsten-halogen or xenon light sources and InGaAs or Si detectors. The spectral resolution was
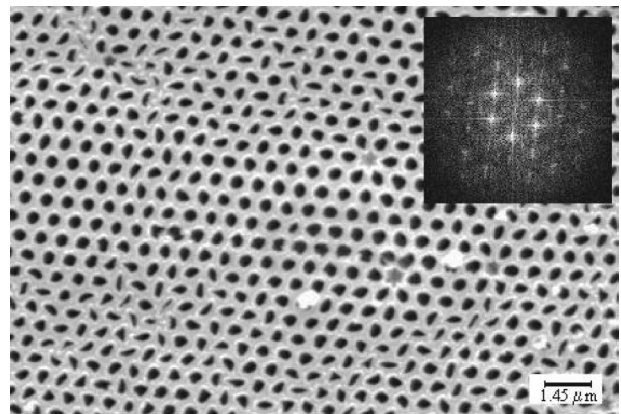
FIG. 1. Scanning electron micrograph of the face of an air-sphere single crystal with $a = 860 \pm 20$ nm (sample No. 439-3). The scale bar is 1.45 μm long. The hexagonal arrangement of voids are an fcc (111) plane. Many peaks in the Fourier transform of the image (inset) confirm the long-range order, that is not disturbed by some local imperfections.
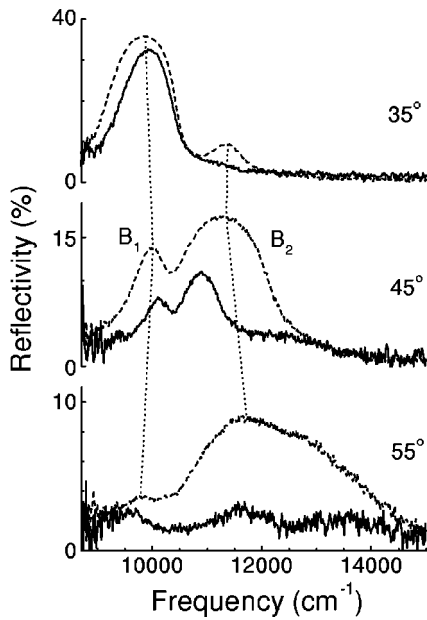
FIG. 2. Bragg-reflection spectra for light incident at angles of 35°, 45°, and 55° for *s* (dashed curves) and *p* polarization (solid curves). The curves are offset, as shown by the left-hand scales. The vertical dotted lines are guides to the eye for the *s*-polarized peaks. B_1 and B_2 label the main peaks in both *s*- and *p*-polarized spectra.

$16\,\mathrm{cm}^{-1}$, the angular resolution $\pm 5°$, and the focal spot 400 μm in diameter. The angle of incidence α is defined as the angle with respect to the [111] surface normal (see Fig. 1). X-ray scattering experiments have revealed that our crystals are oriented predominantly such that the scattering vector lies in the plane spanned by the [111] and [11$\bar{2}$] axes, i.e., the plane through the Γ, U, L, K points of the fcc Brillouin zone of reciprocal space.[5]

Reflectivity spectra were measured up to $\alpha = 75°$. For both polarizations, a single peak, labeled B_1, shifts from $8700\,\mathrm{cm}^{-1}$ at $\alpha = 0°$ to about $10\,000\,\mathrm{cm}^{-1}$ at $\alpha = 30°$, in agreement with simple Bragg diffraction. As Fig. 2 shows, the peak becomes narrower and weaker between $\alpha = 35°$ and 55°, and even decreases in frequency at higher α. Starting at $\alpha = 30°$, a new peak, called B_2, appears at $11\,400\,\mathrm{cm}^{-1}$. It first shifts down and then up in frequency, while becoming stronger and broader. There is also evidence for a weak peak near $13\,500\,\mathrm{cm}^{-1}$ at higher angles. The different polarizations show striking differences: for *s* polarization, B_2 appears at a lower angle, and at $\alpha = 45°$ this peak has a $400\,\mathrm{cm}^{-1}$ higher frequency, a larger width and a higher amplitude compared to *p polarization*. Beyond 55° a single broad peak occurs in the *s*-polarized spectra while the *p*-polarized peaks disappear. The overall decrease of the *p*-spectra amplitudes relative to those of the *s* spectra are probably due to the air-crystal boundary conditions for the electric and magnetic fields.[3] The depolarization of the reflected beams was determined to be less than 1%, consistent with the cubic symmetry of the crystals, hence the effects of disorder on the Bragg peaks are small. The fact that the peaks do not reach ideal (100%) reflectivity and do not exhibit an ideal plateau profile[9] is probably caused by a weak mosaic spread as well as diffuse scattering. Regardless of these details, the observed phenomena cannot be explained with well-known Bragg diffraction.[9,12]
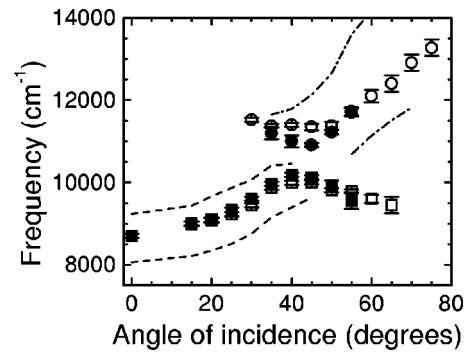
FIG. 3. Center frequencies of Bragg peaks in wave numbers as a function of angle of incidence. Open symbols are *s*- and closed symbols are *p*-polarized data, squares are B_1 peaks and circles B_2 peaks, and the estimated error bars of the peak centers are indicated. The dashed curves are the half heights of the B_1 peaks and the dash dotted curves the half heights of the B_2 peaks, for *s* polarization.

Figure 3 shows the center frequencies of all peaks as a function of α and demonstrates that the frequencies of B_1 and B_2 display an avoided crossing centered at $10\,500\,\mathrm{cm}^{-1}$. Experiments on different crystals with $a \sim 490$ nm revealed the onset of an avoided crossing centered near $18\,000\,\mathrm{cm}^{-1}$. Thus, the frequency ranges of the avoided crossings are inversely proportional to the lattice constants of the crystals, which implies that a Bragg diffraction phenomenon is at the basis of the observations. Figure 3 also shows the full widths at half maximum of the reflection peaks, that gauge the widths of stop gaps in the dispersion relations.[13] The large frequency separations between the peaks in the avoided crossing region is similar to the widths of the peaks, a characteristic of coupled wave phenomena.

To illustrate conceptually the physics behind the coupling phenomenon, Figure 4 shows a cross section of the first Brillouin zone of the fcc structure, the surface associated with Bragg diffraction.[5] The plane displayed is the one relevant to our experiments and includes the high-symmetry points Γ, L,
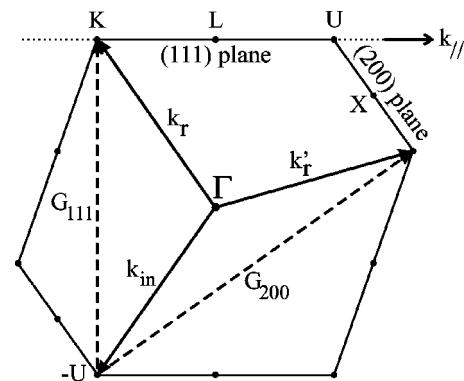
FIG. 4. Cross section of the first Brillouin zone of an fcc structure. Dots indicate high symmetry points Γ, K, L, U, and X. The (111) and (200) Bragg planes are indicated as solid lines on the surface of the first Brillouin zone and by dotted lines on the second zone. $k_{//}$ is the wave vector parallel to the crystal surface in the experiments. The incident wave vector $\mathbf{k}_{in}$ along the Γ to -U direction gives rise to multiple diffraction: $\mathbf{k}_r$ is the wave vector diffracted to the (111) plane and $\mathbf{k}'_r$ is diffracted to the (200) plane. Dashed vectors are $\mathbf{G} = (111)$ and $\mathbf{G} = (200)$ diffraction vectors.

U, and *K*. For simple diffraction from real space (111) planes, the incident ($\mathbf{k}_{\text{in}}$) and reflected wave vectors ($\mathbf{k}_r$) lie on parallel (111)-type faces of the zone surface, with $\mathbf{k}_r = \mathbf{k}_{\text{in}} + \mathbf{G}$, with $\mathbf{G}$ the $hkl = 111$ reciprocal lattice vector. The angle α *inside* the crystal is equal to the angle between $\mathbf{k}_r$ and Γ-L, or to the angle between $\mathbf{k}_{\text{in}}$ and a vector from Γ to -*L*. Diffraction occurs on the surface of the first Brillouin zone, for small α, and moves into the second zone as $\mathbf{k}_{\text{in}}$ moves beyond the -*U* point with increasing α. If $\mathbf{k}_{\text{in}}$ passes through the -*U* point (for intermediate α), two diffracted wave vectors appear simultaneously: $\mathbf{k}_r$ on the (111) Bragg plane and $\mathbf{k}'_r$ on the (200) plane.[16] In multiple Bragg diffraction, the diffracted waves are coupled, hence both diffraction processes are modified compared to simple Bragg diffraction. The occurrence of two (or more[18]) coupled Bragg diffraction processes accounts for our experimental observations.

To quantitatively analyze the multiple Bragg diffraction for our strongly photonic crystals, we have calculated the photonic dispersion curves by solving the macroscopic Maxwell equations using the well-known expansion of vector plane waves.[20,21] The dielectric function for the crystal is represented by $\varepsilon(\mathbf{r}) = \Sigma \epsilon_{\mathbf{G}} \exp(i\mathbf{G}\cdot\mathbf{r})$, where the sum extends over all reciprocal lattice vectors $\mathbf{G}$. Each of the eigenmodes for frequency ω and wave vector $\mathbf{k}$ is represented as $E_{\mathbf{k}}^{\omega}(r,t) = \exp(-i\omega t)\Sigma E_{\mathbf{k},\mathbf{G}}^{\omega} \exp[i(\mathbf{k}-\mathbf{G})\cdot r]$. Using a variety of analytical models for $\varepsilon(\mathbf{r})$, we find that the dispersion relations of the low-frequency modes relevant for this work can be computed with *only three* distinct ϵ_G, viz., ϵ_0, $\epsilon_{(111)}$, and $\epsilon_{(200)}$ (along with their symmetry related equivalents);[19] i.e., frequencies are found within 5% of converged results obtained with 663 plane waves. The essence of this surprising result is that the small number of necessary modes $E_{\mathbf{k},\mathbf{G}}^{\omega}$ allows for a detailed analysis of the physics of our observations.

The actual photonic dispersion curves for our crystals are computed with an empirical approach similar to the well-known methods used to obtain electronic band structures in semiconductors,[22] because a number of *ab initio* models for $\varepsilon(\mathbf{r})$ (Ref. 21) correspond only approximately to the structure and titania filling fraction of our samples, see Fig. 1 or Ref. 15. We take $\epsilon_0 = 1.41$ from the square of the effective refractive index.[17] The $1200\,\text{cm}^{-1}$ width of the Bragg peak at $\alpha = 0°$ fixes $\epsilon_{(111)} = -0.18$. We have chosen $\epsilon_{(200)} = 0.1\epsilon_{(111)}$, guided by a model of close-packed air spheres,[21] although variations of this coefficient by 50% shift the dispersion curves less than 5%. Figure 5 presents the calculated dispersion curves for the six lowest frequency Bloch modes as a function of the wave vector along the *L*-*U* direction.[23,24] By momentum conservation parallel to the crystal surface, this wave vector equals the wave vector of the incident light parallel to the crystal surface $k_{//}$ in the experiments (see Fig. 4).

For comparison with theory, we also plot in Fig. 5 the reflectivity center frequencies of Fig. 3 as a function of $k_{//}$, where $k_{//} = (\omega/c)\sin\alpha$. It is clear from Fig. 5 that the main features of the model show a remarkable agreement with the experimental data: the most dramatic point is the clear avoided crossing between the peaks B_1 and B_2 which is quantitatively described by the theoretical dispersion bands.
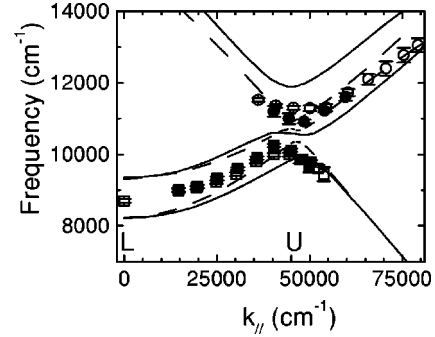
FIG. 5. Dispersion relations of low-frequency Bloch states as a function of wave vector $k_{//}$ along the *L*-*U* direction, see Fig. 4. The *L* and *U* points are indicated. Solid curves are calculated *s* modes and dashed curves are *p* modes. Circles indicate the B_1 peaks and squares the B_2 peaks, open symbols are for *s*-polarized light and closed symbols for *p* polarization.

Detailed analysis of the eigenfunctions $E_{\mathbf{k}}^{\omega}(r,t)$ shows that the two pairs of *s* and *p* bands that move up from near $9000\,\text{cm}^{-1}$ at $k_{//} = 0\,\text{cm}^{-1}$ to $13\,000\,\text{cm}^{-1}$ at $k_{//} = 80\,000\,\text{cm}^{-1}$, in essence delimit the stop band due to (111) Bragg reflection. The two single *s* and *p* bands that move from $14\,000\,\text{cm}^{-1}$ at $k_{//} = 20\,000\,\text{cm}^{-1}$ down to $8000\,\text{cm}^{-1}$ at $k_{//} = 70\,000\,\text{cm}^{-1}$ are mainly $E_{\mathbf{k},\mathbf{G}}^{\omega}$ modes with $\mathbf{G} = (200)$. Near the *U* point, the lower edge of the low-*k* (111) stop band splits off to become the (200) band. As a result, the (111) stop band undergoes major changes: the stop gap ceases to exist in agreement with the disappearance of B_1, the center frequency turns over and the width decreases, and the s-components shift down in frequency relative to the *p* bands, all of which are seen experimentally (see Fig. 2). Near the *U* point, the (200) modes join the upper edge of the low-*k* (111) stop band to form a new stop band, that is experimentally observed as B_2. At the crossing, it is seen that the theoretical *s*-stop band has a higher center frequency than the *p*-stop band, in agreement with the experiments. At large wave vectors, the experimental frequencies are somewhat lower than the center of the stop band, which may be partly a projection effect of $k_{//}$, and partly because $E_{\mathbf{k},\mathbf{G}}^{\omega}$ modes with other $\mathbf{G}$'s become important at high frequencies. The frequency gap between the lower and higher frequency Bragg peaks, and the appearance of multiple peaks, is a clear consequence of the coupling of Bloch waves along the edge of the first Brillouin zone (*U*-*W*-*K*). These effects are manifestations of properties of a 3D photonic crystal that clearly cannot be understood within the framework of single Bragg diffraction wherein two coupled waves cause a single Bragg peak.[9,12]

The large dielectric contrast of our crystal induces multiple Bragg diffraction for light with avoided crossing behavior over tens of degrees, about 10^6 more than for x rays. In our case this amounts to modified light propagation for $\sim 40\%$ of all directions at the relevant frequencies. The coupled diffraction considerably flattens the photonic bands on the surface of the Brillouin zone and keeps stop gaps at the same frequencies (Fig. 5), leading to grossly altered density of states and spontaneous emission characteristics. Ultimately, optical multiple diffraction leads to a frequency range for which light propagation is inhibited for *all* polar-

izations and directions: a photonic band gap.[1,3,4] While multiple Bragg diffraction has been observed earlier with x rays,[16] the physics and consequences differ vastly from multiple diffraction of light in photonic crystals, besides the obvious difference of 10^4 in wavelength: the interaction of x rays with arrays of individual atoms is described by the microscopic Maxwell equations,[25] and the interaction is extremely weak ($\sim 10^{-5}$ compared to the optical regime), thus fulfilling one of the basic approximations of the dynamical diffraction theory, and allowing accurate predictions with scalar waves.[16] Subtle avoided crossings of only arc seconds appear for x rays, hence the density of states is the equal to the one for free photons[4] to within $\sim 10^{-4}$ and no x-ray photonic band gap is expected.

Finally, we note that multiple Bragg diffraction must not be confused with multiple scattering.[26] The differences between the two phenomena can be illustrated by the following examples: (i) multiple scattering can readily occur with simple Bragg diffraction, i.e., if the diffracted beam is rediffracted many times by a single set of crystal planes. This case is considered in the dynamical diffraction theory[9] and is at the heart of the models in Ref. 12. (ii) The intensities observed in multiple x-ray diffraction experiments are often well described in the kinematical treatment, that is, for vanishing photonic interaction.[16] In this paper, multiple diffraction occurs in the limit of strong photonic interaction, hence strong multiple scattering.

---

*Permanent address: Department of Physics, University of Toronto, Toronto, Canada M5S 1A7.

†Email: wvos@wins.uva.nl; web: www.wins.uva.nl/research/scm

[1] E. Yablonovitch, Phys. Rev. Lett. **58**, 2058 (1987); S. John, *ibid.* **58**, 2486 (1987).

[2] B. Goss Levi, Phys. Today **52(1)**, 17 (1999); D. Normile, Science **286**, 1500 (1999).

[3] J.D. Joannopoulos, R.D. Meade, and J.N. Winn, *Photonic Crystals* (Princeton University Press, Princeton, NJ, 1995).

[4] *Photonic Band Gap Materials*, edited by C.M. Soukoulis (Kluwer, Dordrecht, 1996).

[5] N.W. Ashcroft and N.D. Mermin, *Solid State Physics* (Holt, Reinhart and Winston, New York, 1976).

[6] H. DeNeve *et al.*, Appl. Phys. Lett. **70**, 799 (1997).

[7] H. Kosaka *et al.*, Phys. Rev. B **58**, 10 096 (1998).

[8] O. Painter *et al.*, Science **284**, 1819 (1999).

[9] R.W. James, *The Optical Principles of the Diffraction of X-Rays* (Bell, London, 1954).

[10] Fine structures with line uncrossings and splittings have been observed in Kossel rings of dilute colloidal crystals by T. Yoshiyama and I.S. Sogami, Phys. Rev. Lett. **56**, 1609 (1986), but were not interpreted in the context of photonic band gap crystals.

[11] J.G. Fleming and S.-Y. Lin, Opt. Lett. **24**, 49 (1999); S. Noda, N. Yamamoto, H. Kobayashi, and M. Okano, Appl. Phys. Lett. **75**, 905 (1999).

[12] See e.g.: R.J. Spry and D.J. Kosan, Appl. Spectrosc. **40**, 782 (1986); K.W.K. Shung and Y.C. Tsai, Phys. Rev. B **48**, 11 265 (1993); V.N. Bogomolov *et al.*, Phys. Rev. E **55**, 7619 (1997); J.F. Bertone *et al.*, Phys. Rev. Lett. **83**, 300 (1999).

[13] M.S. Thijssen *et al.*, Phys. Rev. Lett. **83**, 2730 (1999).

[14] The limited relative spectral range a/λ of Ref. 13 hampered the observation of multiple diffraction.

[15] J.E.G.J. Wijnhoven and W.L. Vos, Science **281**, 802 (1998).

[16] S.-L. Chang, *Multiple Diffraction of X-rays in Crystals* (Springer, Berlin, 1984).

[17] The n_{eff} is obtained from the center frequency at $\alpha = 0°$ and the known 111 spacing, and agrees with a Maxwell-Garnett average, see also W.L. Vos *et al.*, Phys. Rev. B **53**, 16 231 (1996).

[18] For diffraction near the W point, three Bragg planes intersect: (111), (200), and $(1\bar{1}1)$.

[19] The coefficients $\epsilon_{(111)}$ and $\epsilon_{(200)}$ determine Bragg reflection from (111) and (200) planes, respectively.

[20] K.M. Ho, C.T. Chan, and C.M. Soukoulis, Phys. Rev. Lett. **65**, 3152 (1990).

[21] H.S. Sözüer, J.W. Haus, and R. Inguva, Phys. Rev. B **45**, 13 962 (1992); K. Busch and S. John, Phys. Rev. E **58**, 3896 (1998).

[22] See, E.O. Kane in *Handbook on Semiconductors*, edited by W. Paul (North Holland, New York, 1982), Vol. 1, p. 193.

[23] We consider eigenmodes in the L-U-W plane (with $k_x, k_y, k_z > 0$) as superpositions of six plane wave components with **G** $= (000)$, (111), $(1\bar{1}\bar{1})$, (200), $(11\bar{1})$, and $(1\bar{1}1)$. The first four are needed to quantitatively represent the dispersion curves, and the latter two allow one to preserve the mirror symmetry and hence (s,p)-polarization symmetry of the dispersion curves with respect to the Γ-X-U plane, since the L-U trajectory is on the (Γ-L-U) mirror symmetry plane.

[24] Modes on the L-U trajectory have the same dispersion relations as on the L-K trajectory, on account of Bloch's theorem, see Ref. 5.

[25] J.D. Jackson, *Classical Electrodynamics* (Wiley, New York, 1999).

[26] P. Sheng, *Introduction to Wave Scattering, Localization, and Mesoscopic Phenomena* (Academic, San Diego, 1995).